



## **The role of retained austenite on the formation of the nanostructured hard-turned induced white layer in AISI 52100 bearing steel**

Downloaded from: <https://research.chalmers.se>, 2024-07-17 11:48 UTC

Citation for the original published paper (version of record):

Kokkiralala, S., Osman, K., Holmberg, J. et al (2024). The role of retained austenite on the formation of the nanostructured hard-turned induced white layer in AISI 52100 bearing steel. *Procedia CIRP*, 123: 292-297.  
<http://dx.doi.org/10.1016/j.procir.2024.05.052>

N.B. When citing this work, cite the original published paper.

7<sup>th</sup> CIRP Conference on Surface Integrity

# The role of retained austenite on the formation of the nanostructured hard-turned induced white layer in AISI 52100 bearing steel

S. Kokkiralaa<sup>a,\*</sup>, K. Osman<sup>b</sup>, J. Holmberg<sup>b</sup>, S. Kimming<sup>c</sup>, H. Iwasaki<sup>d</sup>, U. Klement<sup>a</sup>, S.B. Hosseini<sup>b</sup>

<sup>a</sup>Industrial and Materials Science, Chalmers University of Technology, SE-412 96 Gothenburg, Sweden

<sup>b</sup>RISE AB, Department of Manufacturing Processes, BOX 104, SE-431 22 Mölndal, Sweden

<sup>c</sup>AB SKF, SE-41550 Gothenburg, Sweden

<sup>d</sup>SUMITOMO ELECTRIC Hartmetall GmbH, Konrad-Zuse-Str. 9, 47877 Willich, Germany

\* Corresponding author. Tel.: +46 734959063; E-mail address: [sahithk@chalmers.se](mailto:sahithk@chalmers.se)

## Abstract

Interest in hard-turning is steadily increasing due to its obvious benefits in terms of desirable surface integrity and improved operational efficiency. Surface microstructural variations can occur during machining due to cutting speed, tool geometry, and process conditions. These variations create nanostructured white layers (WL), categorized as mechanically induced white layers (M-WL) or thermally induced white layers (T-WL). This study explored the role of retained austenite (RA) content (<2%, 12%, and 25%) on WL generation in AISI 52100 bearing steel, offering insights for optimizing hard-turning. The findings showed that, regardless of RA content, samples exhibited M-WL with no dark layer beneath the white layer when utilizing a cutting speed ( $V_C$ ) of 60m/min using a fresh insert. Increasing tool flank wear to 0.2mm led to the formation of T-WL and surface tensile residual stresses in specimens with higher RA content (12% and 25%). This effect was also observed at 260m/min with a fresh cutting insert. Machining at 260m/min with a worn tool ( $V_B$ ) of 0.2mm resulted in T-WL and surface tensile residual stresses, independent of RA content. Additionally, a 0.2mm tool wear caused a significant shift in the maximum subsurface compressive residual stresses to greater depths, irrespective of RA content.

© 2024 The Authors. Published by Elsevier B.V.

This is an open access article under the CC BY-NC-ND license (<https://creativecommons.org/licenses/by-nc-nd/4.0>)

Peer-review under responsibility of the scientific committee of the 7th CIRP Conference on Surface Integrity

**Keywords:** Hard turning; retained austenite; white layers; nanostructured materials; tool wear

## 1. Introduction

Hard Turning is referred to as the machining of hardened steels (> 45HRC) and is performed by a geometrically well-defined single-point cutting tool [1]. Due to its superior flexibility, higher efficiency, and environmentally friendly process, hard turning is a promising substitute for the grinding process in industrial applications [1,2]. The main goal of hard turning is to produce surfaces with higher dimensional precision and better surface integrity, which promotes better functional performances [3]. Hashimoto et al. [4] compared the surface integrity of the hard-turned and ground AISI 52100 and found that equivalent surface roughness ( $R_a = 0.07\mu\text{m}$ ) can be achieved. Importantly, the hard-turned surface had a 100%

longer fatigue life than the ground sample due to the improved surface integrity features. However, the hard turning process is still not yet widely used on an industrial scale. The major concerns are related to tool wear which affects the surface and subsurface microstructural properties by generating tensile residual stresses and higher surface roughness with tool wear [5]. But by controlling the cutting parameters like i) cutting speed ( $V_C$ ), ii) feed rate ( $f$ ), iii) depth of cut ( $a_p$ ), and iv) tool geometry the desired surface integrity properties can be achieved [1,5].

Interestingly, during hard-turning the original tempered martensite on the machined surface transforms into a nanostructure microstructure, which is different from the bulk material and possesses higher hardness due to refined grain

structure [6,7,8]. It is referred to as the “white layer” (WL) since it appears white and featureless when observed through an optical microscope after polishing and etching due to the nanocrystalline grains. The white layer consists of subgrains in the range of 10nm–500nm [4,7,8]. Depending on the formation mechanisms of white layers, even a darker region referred to as “dark layer” (DL) is observed beneath white layers [1].

As studied by Hosseini et al. [9], dark layers underneath the white layers are observed in thermally-induced white layers (T-WL) with the dark layer being 14% softer than the bulk due to the over-tempering of martensite. The white layers consist of equiaxed grains and are formed due to reverse martensitic transformation with higher retained austenite (RA) content. In contrast, in the mechanically-induced white layers (M-WL), no dark layer is observed beneath the white layer and the formation mechanism of the white layer is by dynamic recovery process which results in elongated nano-sized grains [8]. The hardness in the white layers is ~26% higher than in the base material with reduced retained austenite content and no dark layer beneath the white layer suggesting the possibility of possessing improved wear and mechanical properties.

Most hard-turning studies conducted to understand the formation and properties of white layers have been performed on through-hardened bearing steels with approximately 0-2% retained austenite [10,11]. Carburized steel on the other hand consists of varying amounts of retained austenite (typically 10%-30%) depending on the applications. For example, due to their better surface wear resistance and tougher subsurface, they are often used in the transmission system (gears, shafts) of automobiles [12]. Unfortunately, the effect of retained austenite on WL formation and its resulting surface integrity on carburized steel didn't receive the required attention in the research field of hard turning.

RA which is present in carburized steel when subjected to thermo-mechanical loads, undergoes a phase transformation from the austenite phase ( $\gamma$ ) to epsilon carbide ( $\epsilon$ ) and  $\alpha'$  martensite phase. It occurs through deformation which in combination with grain refinement leads to an increase in microhardness on the surface, increased dislocation density, and deformation twinning [13,14].

Bedekar et al. [3] studied the effect of varying tool geometry on hard-turning carburized SAE 8620 steel containing 30% RA. By lowering the cutting speed ( $V_C$ ), the RA fractions reduced significantly for both the negative and positive rake angle inserts indicating the possibility of strain-induced martensitic transformation. A higher reduction of RA% at lower  $V_C$  is observed for the worn inserts due to excessive mechanical loads causing severe plastic deformation on the machined surface. By machining with higher  $V_C$ , due to the reverse martensitic transformation, increased RA fractions were observed in the new and worn inserts.

However, there is a lack of information regarding the generation of the nanostructured white layer either M-WL or T-WL in AISI 52100 steel with different RA content during hard turning.

From the above-mentioned literature, white layer formation during hard-turning is a common phenomenon observed on AISI 52100 bearing steel. Depending on the varying cutting parameters, the formation of the white layer can be either

mechanically induced or thermally induced. The main objective of this investigation is to understand the influence of retained austenite contents in the formation of white layers and their impact on residual stresses.

## 2. Materials and Methods

### 2.1. Workpiece material

The workpiece material used in the study is AISI 52100 chromium-containing high carbon steel grade with the chemical composition shown in Table 1. The through-hardened <2% RA samples are industrially available [15]. To obtain tempered martensitic microstructure with two different RA fractions (12%, 25%), the AISI 52100 steel was heat treated according to Fig. 1. Batch 1 (12% RA) samples were pre-heated at 400°C for 120 minutes followed by a subsequent austenitization at 860°C for 120 minutes with a carbon potential of 0.75%. Batch 2 (25% RA) was austenitized at 920°C using a carbon potential of 0.8% for 120 minutes. Both batches were quenched in oil with samples placed vertically to attain homogeneity at 80°C and then washed. The post quenching process was carried out at 5-8°C for 30 minutes and then both batch samples were tempered at 160°C for 60 minutes. After the heat treatment process, the final hardness of the 3 batches is  $61 \pm 2$ HRC with different RA content (<2%, 12% & 25%).

Table 1. AISI 52100 chemical composition (wt. %) [2]

Fe	C	Mn	Si	Cr	S	P
Bal.	0.95	0.32	0.26	1.42	0.001	0.009

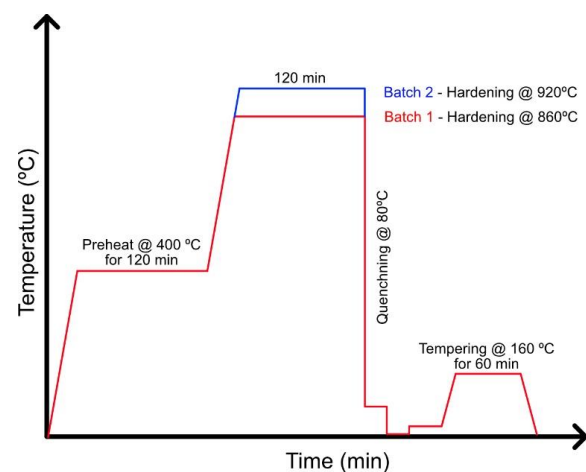


Fig. 1. Heat treatment conditions to generate 2 batches of varying retained austenite fractions.

### 2.2. Hard turning

The hard turning tests were performed on the Hemburg machine using a polycrystalline cubic boron nitride (PcBN) coated BNC 200 tool insert (DNGA 150612 (HS)) with a 1.2mm nose radius. The experiments were performed on a cylindrical rod with a length of 200mm and a diameter of 34mm. For the tests, the cutting speed ( $V_C$ ) and tool wear ( $V_B$ ) were varied in 2 levels whereas the feed rate ( $f$ ) and depth of

cut ( $a_p$ ) were kept constant with 0.16mm/rev and 0.16mm using flooding coolant. In total 12 hard turning tests were conducted.

Table 2. Varying parameters for the current study

Factors	$V_c$ (m/min)	$V_B$ (mm)
Low	60	Fresh
High	260	0,2

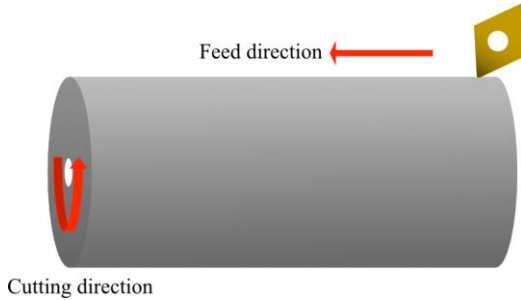


Fig. 2. Feed direction and cutting direction on the generated samples.

### 2.3. Characterization methods

Stresstech XSTRESS 3000 G2R X-ray diffractometer was used to measure the surface and subsurface residual stress profiles with a Cr-K $\alpha$  source and a 2mm collimator. The residual stresses were measured with the Sin<sup>2</sup>( $\psi$ ) method with tilt angles ranging from -45° to +45° which measures the lattice spacing and strain was calculated. A total of 5 measurements (0, 10, 30, 50, 100  $\mu$ m) were done until 100 $\mu$ m from the machined surface by performing electropolishing using saturated salt electrolyte to remove the material layer by layer.

Microstructural features were characterized using a Zeiss Axioscope 7 light optical microscope (LOM) and Zeiss Gemini 450 scanning electron microscope (SEM). The sample preparation was done by hot mounting the cut sample in 40mm polyfast Bakelite diameter material and polished until 1 $\mu$ m diamond suspension to have a scratch-free sample. The polished mounted samples were etched with 2% nital etchant to proceed with the investigation.

## 3. Results

### 3.1. Residual stresses

The hard-turned machined surfaces with measured residual stress depth profiles along the feed and cutting direction are shown in Figs. 3 - 6. Along the feed direction with a low cutting speed of 60m/min (see Fig. 3), the surface residual stresses for the fresh inserts with different retained austenite content are in the similar range between -700MPa to -600MPa. As the tool wear increased, the surface compressive stresses decreased but the higher RA content samples showed better values in comparison to the <2% RA sample. In the subsurface range, higher RA content with high tool wearsamples observed higher compressive stresses. By increasing the cutting speed to 260m/min using fresh inserts (Fig. 4), <2% RA content sample exhibited higher surface and subsurface compressive stresses. For higher tool wear, high surface tensile stresses of around 150MPa are observed in the 25% RA sample.

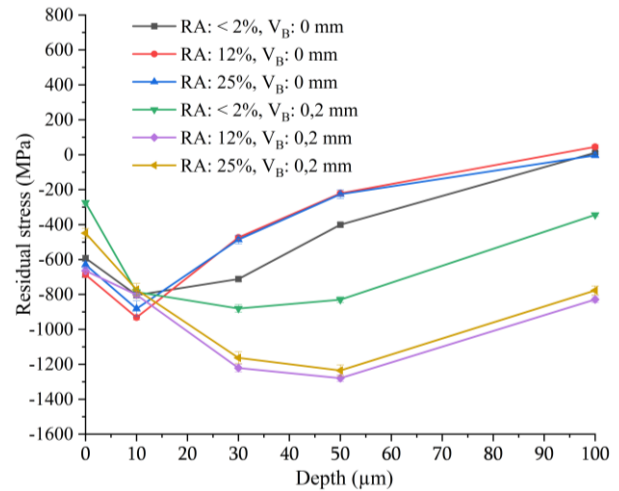


Fig. 3. Residual stresses measured along the feed direction for varying retained austenite fractions and tool wear with constant  $V_c$ : 60m/min.

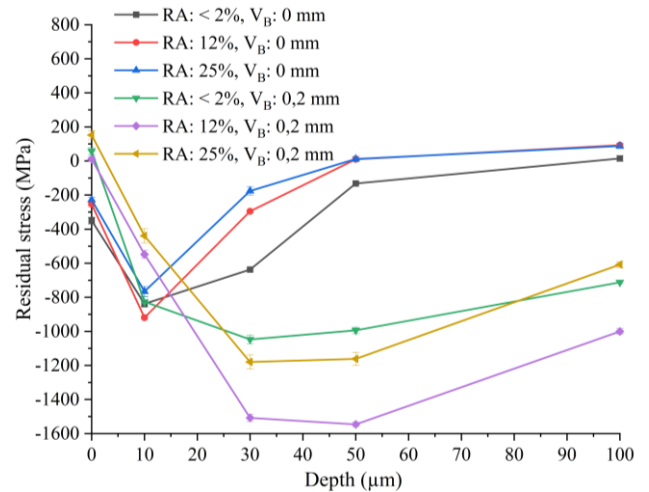


Fig. 4. Residual stresses measured along the feed direction for varying retained austenite fractions and tool wear with constant  $V_c$ : 260m/min.

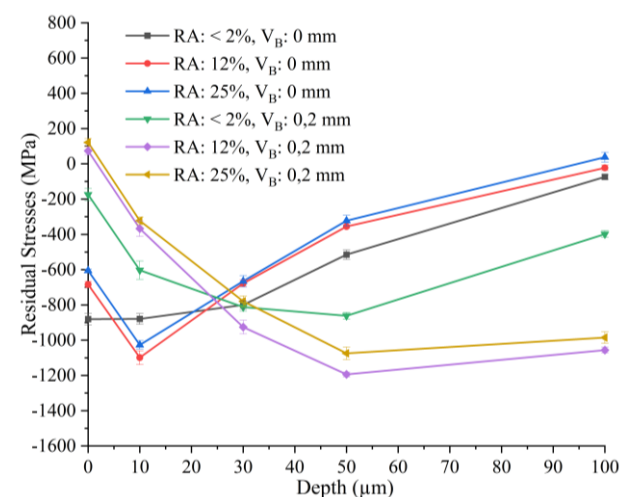


Fig. 5. Residual stresses measured along the cutting direction for varying retained austenite fractions and tool wear with constant  $V_c$ : 60m/min.

As the cutting speed increased, the surface compressive stresses decreased by about 300MPa for fresh inserts and observed tensile stresses of 20MPa to 150MPa for the worn inserts.



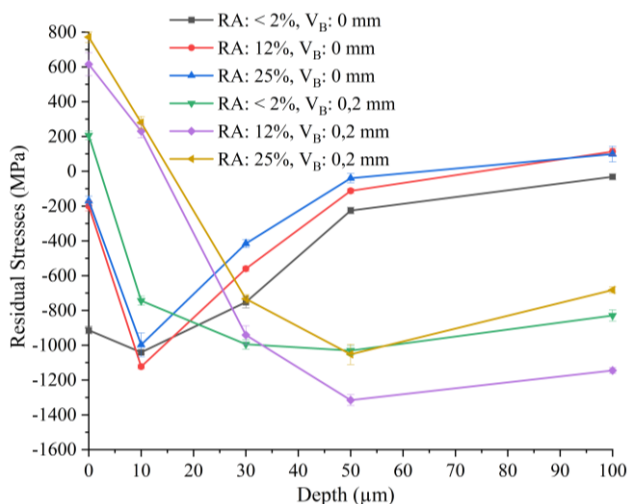


Fig. 6. Residual stresses measured along the cutting direction for varying retained austenite fractions and tool wear with constant  $V_c$ : 260m/min.

For both the cutting speeds, irrespective of the different retained austenite content, higher tool wear samples observed higher compressive stresses at the greater depths of around  $30\mu\text{m} - 50\mu\text{m}$  as an effect of the increased contact area of the tool on the workpiece generating higher mechanical loads and eventually shifting the compressive depths.

Along the cutting direction, for the low cutting speed of 60m/min as observed in Fig. 5, higher surface compressive stresses are observed with <2% RA fraction samples compared to the 12% and 25% RA content samples for both fresh and worn inserts. This indicates that the higher retained austenite fractions promote the reduction of compressive stresses and in the case of worn inserts both the 12% and 25% RA samples observed surface tensile stresses around 70MPa to 110MPa in comparison to the -180MPa surface compressive stress for the <2% RA sample. In the subsurface region and with the fresh inserts, <2% RA sample observed lower compressive stresses. But in the case of worn inserts, around  $30\mu\text{m}$  from the surface, 12% and 25% RA content observed better compressive stresses than <2% RA.

A similar trend is observed with 260m/min along the cutting direction as seen in Fig. 6. The <2% RA samples observed better surface residual stresses when using both the fresh and worn inserts. In the case of worn inserts, all samples with different RA content observed surface tensile stresses reaching a maximum of 800 MPa for 25% RA sample and 205MPa for <2% RA sample. The worn insert samples observed shallower subsurface compressive stresses for different RA content samples indicating the huge influence of tool wear on the residual stress profiles. The differences between the residual stress profiles of the 12% and 25% RA samples are not huge in comparison to the samples machined with <2% RA residual stress profiles. However, it is observed that increasing the RA content promotes the reduction of compressive stresses along the cutting direction from the temperature influence.

### 3.2. Microstructure

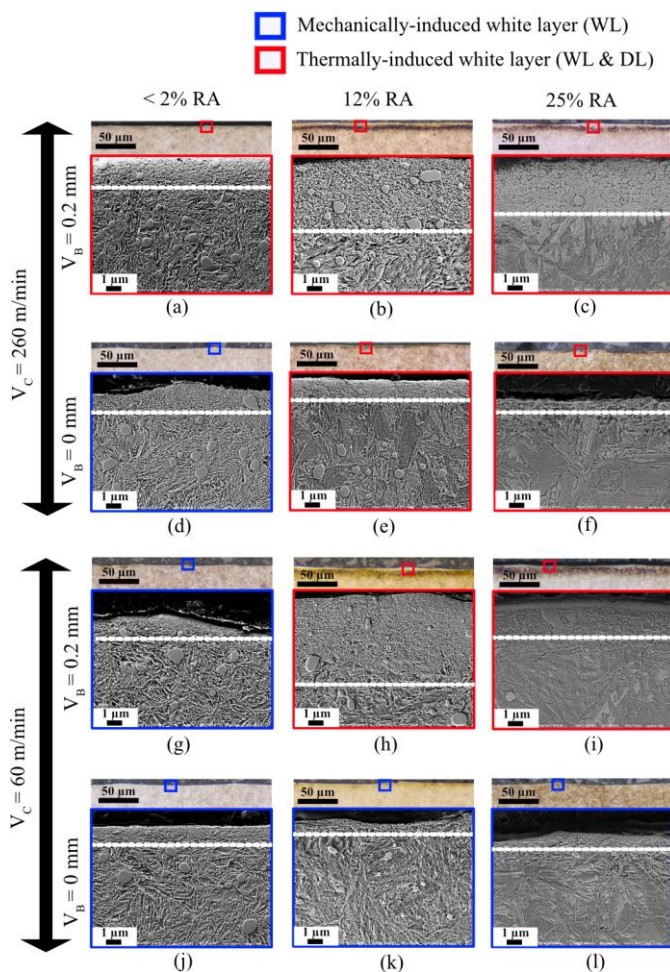


Fig. 7. Light optical microscopy (LOM) images of 12 parameters indicating the white and dark layer and respective scanning electron images of the LOM images. The white dashed line indicates the boundary of the white layer region from the bulk for the mechanically-induced white layer and the dark layer for the thermally-induced white layer.

Fig. 7 shows the microstructural features of the 12 samples examined in the current study. For all the conditions, the white layer formation is observed but with different thicknesses and in some cases as discontinuous white layers. The morphology of the white layer is observed above the dashed white line in the SEM images, also illustrating the thickness of the white layer from the machined surface, and it appears as a white featureless layer in the LOM images. The blue box indicates the formation of a mechanically-induced white layer (M-WL) and the red box indicates the thermally-induced white layer (T-WL). The differentiation is made by observing the formation of a dark layer beneath the white layer with M-WL generating only the white layer and the T-WL generating both white and dark layers on the machined surface.

With the low cutting speed of 60m/min and using fresh insert, all the samples with different retained austenite content showed M-WL with a similar thickness of  $1\mu\text{m}$  as seen in Figs. 7(j-l). The microstructure morphology is different in these samples due to different RA content and  $(\text{Fe}, \text{Cr})_3\text{C}$  carbide particles.

By increasing the tool wear to 0.2mm with a similar low cutting speed of 60 m/min, the <2% RA sample generated M-WL while high RA content samples (12% & 25%) generated T-WL with dark layers beneath the white layers as observed in Figs. 7(g-i). The 12% RA sample showed higher WL thickness and the 25% RA sample observed a larger DL thickness.

Increasing the cutting speed to 260m/min and using fresh inserts (Fig. 7(d-f)) led to T-WL with dark layers beneath for higher RA fraction samples. The <2% RA sample showed a M-WL with no dark layer. Finally increasing the tool wear to 0.2mm and with a cutting speed of 260m/min, all the 3 samples generated T-WL as seen in Figs. 7(a-c). However, the <2% RA sample in Fig. 7(a) generated very thin DL beneath the WL compared to the 12% and 25% RA samples, and the surface tensile residual stress of about 200MPa as observed in Fig. 6 indicates a rise in surface temperature. For all the fresh insert samples, the WL thickness is comparable. However, in the case of worn inserts, the 12% RA sample shows a larger WL thickness, but this is due to the selected area in the image. As observed from LOM, the thickness isn't constant and varies by hundreds of nanometers due to the tool wear micro geometry. This indicates that the higher retained austenite contents are promoting the formation of T-WL with higher temperature influence and a similar observation is made for the above residual stresses.

## 4. Discussion

### 4.1. Role of retained austenite.

In hard-turning, the sample surfaces experience excessive thermo-mechanical loads. Depending on whether the thermal or mechanical energy is dominating, it is possible that the surface can predominantly experience phase transformation or severe plastic deformation. Consequently, the generated white layer will feature different characteristics. Depending on the morphology of the white layer observed from the LOM, M-WL and T-WL are differentiated [9]. For example, the M-WL samples that were characterized by surface compressive stresses were generated at temperatures below the austenitization temperature. The formation mechanism is dynamic recovery, where the severe plastic deformation results in the elongated sub-grain structure or breakage of grains that orient along the shear direction [8, 9, 16]. The resulting microstructure contains nanocrystalline grains in the range of a few tens to hundreds of nanometers in the white layer region and underneath no dark layer is observed. In the case of T-WL, the samples generated surface tensile residual stresses governed by the high cutting temperatures well above the  $A_{c1}$  temperature line. The T-WLs are formed through the advancement from dynamic recovery to dynamic recrystallization as the temperature rapidly progresses to above  $A_{c1}$ . This enables the nucleation of new grains by accommodating dislocations from highly deformed elongated grains. It finally leads to equiaxed nanocrystalline grains in WL with dark layers beneath them consisting of over-tempered martensite [6-9].

In the current study, it was observed that by increasing the RA content, the formation of T-WL is preferred. In addition,

the combined effect of increased RA content, tool wear, and cutting speed leads to thicker T-WL. For example, at low cutting speed, i.e., 60m/min and when using a fresh cutting tool, M-WLs were observed, even for the specimens with higher RA content. This is due to the dominant mechanical effect at a low cutting speed of 60m/min. As the RA is metastable, higher RA content samples (12% and 25%) undergo deformation-induced martensitic transformation [21]. At the lowest cutting speeds, i.e.,  $V_C$ : 60m/min, as the tool wear increased to  $V_B$ : 0.2mm surface compressive residual stresses and M-WL were measured on the specimens with <2% RA, whereas the specimens containing 12% and 25% RA resulted in surface tensile residual stresses and T-WL.

Similar observations are seen with  $V_C$ : 260m/min and using a fresh insert. Specimens with low retained austenite content i.e., <2% RA, M-WL, and surface compressive stresses were measured, whereas for the specimens 12% RA and 25% RA T-WL were found after machining. As  $V_B$  increased to 0.2 mm at  $V_C$ : 260m/min, T-WL and surface tensile stresses of varying magnitudes were measured for all specimens. As reported by Hosseini et al. [17] utilizing similar BNC 200 cutting tool geometry and for <2% RA tempered martensitic material, T-WL is generated within the cutting temperature range of 840°C to 940°C. The M-WL is formed approximately at 550°C with the austenitization temperature at around 750°C. This indicates that higher RA content (12% and 25%) proceeds predominantly above the transformation temperature under similar cutting conditions that produce T-WL.

The general trend in residual stresses from Fig. 3 to Fig. 6 represents a “hook shape” profile independent of RA content, tool wear, and cutting speed [18]. As the  $V_C$  increases, the compressive stresses move towards the tensile range which is related to the heat generation at the machined surface. The increase in tool wear induces a temperature rise and shifts the maximum compressive stresses to a larger subsurface due to plastic deformation caused by material softening [10]. For 60m/min and 260m/min using the fresh insert, <2% RA sample has higher compressive stresses in the subsurface region due to the higher martensite content. In contrast for  $V_B$ : 0.2mm, 12%, and 25% RA content samples generated high compressive stresses in the subsurface due to the deformation-induced martensitic transformation. The plastic strain caused by the hard-turning transforms the retained austenite to martensite.

The metastable RA phase when subjected to thermo-mechanical loading transforms depending on its thermal and mechanical stability [19, 20]. Also as reported by Hosseini et al [17], the hard-turning process will change the austenitization temperature due to the high heating rates, contact pressure, plastic strain, and alloying elements. Hence it can be considered that the different heat treatments used in the present study will also have a significant contribution to the WL formation and its characteristics. For example, the carbon content and the prior austenite grain size are different for 12% and 25% RA content when compared to the <2% RA content sample. Also, the carbide concentration is lower for high RA samples as seen in Fig.7. As the temperature/time is increased during austenitization, a larger volume fraction of the primary (Fe, Cr)<sub>3</sub>C-carbides dissolves resulting in a higher carbon concentration in the austenite, which retains higher austenite

upon quenching. The increase in carbon concentration lowers the martensite start temperature retaining a higher content of austenite. Banerjee [22] observed a similar behavior of higher RA content by increasing the austenitization temperature. The influence of specific cutting pressure on the austenitization temperature is significant. The austenite phase (FCC) being denser than tempered martensite (BCC) concerning the atomic packing fraction will reduce the austenitization temperature due to the cutting pressure effect [10,21]. A similar observation was seen in the current work as the higher RA content (12% and 25%) samples generated T-WL in contrast to the <2% RA sample which generated M-WL for similar cutting conditions except for  $V_C$ : 260m/min and  $V_B$ : 0.2mm where all the three RA content observed T-WL with varying intensities.

The machining process is a combined effect of strain and temperature influence. Depending on the cutting parameters, it generally occurs in the time range of  $10\mu\text{s} - 500\mu\text{s}$ . In these conditions, the carbon content, prior austenite grain size, RA morphology, and pressure effects due to the increased RA content influence the reduction of austenitization transformation temperature [20]. However, to fully understand the underlying mechanisms of how the retained austenite affects the WL formation, and its final characteristics, a detailed investigation of the austenitization temperature is necessary. In such work, the influence of heating rate, strain, pressure, and carbon concentration must be included [18].

## 5. Conclusions

The role of retained austenite (RA) in generating the nanostructured WL for AISI 52100 steel was investigated with three different levels, i.e. <2%, 12%, and 25%.

When machined at 60m/min using fresh cutting inserts, independent of the RA content, M-WLs accompanied with surface compressive residual stresses were observed. As the tool flank wear increased to 0.2mm, the specimens with higher RA content, i.e. 12% and 25% resulted in the formation of T-WL which was accompanied by surface tensile residual stresses. A similar observation was made when machining at 260m/min using a fresh cutting insert.

Machining at 260m/min with a worn cutting tool,  $V_B$ : 0.2mm, independent of the RA content, all surfaces were characterized by T-WL that was accompanied by surface tensile residual stresses. Moreover, the tool wear of 0.2mm resulted in a significant shift of the maximum subsurface compressive residual stresses to larger depths beneath the machined surface. The shift of the position of the maximum compressive residual stresses was observed independent of the RA content.

## Acknowledgments

The study is part of the Turn2Flex (*Vinnova 2021-01274*) project and the HybridSurf (*Vinnova 2018-04263*) project financed by the Swedish government agency for Enterprise and Innovation. We especially thank AB SKF, Ovako AB, and Sumitomo Electric Hartmetall GmbH for supporting with machining and material support.

## References

- [1] Hosseini SB, Rytberg K, Kaminski J, Klement U. Characterization of the Surface Integrity Induced by Hard Turning of Bainitic and Martensitic AISI 52100 Steel. *Procedia CIRP* 2012;1:494-499.
- [2] Zhang X, Huang X, Chen L, Leopold J, Ding H. Effects of Sequential Cuts on White Layer Formation and Retained Austenite Content in Hard Turning of AISI52100 Steel. *ASME. J. Manuf. Sci. Eng.* June 2017; 139:6.
- [3] Bedekar V, Shivpuri R, Chaudhari R, Scott Hyde R. Nanostructural evolution of hard turning layers in response to insert geometry, cutting parameters and material microstructure. *CIRP Annals* 2013; 62:1. p. 63-66.
- [4] Hashimoto F, Guo YB, Warren AW. Surface Integrity Difference between Hard Turned and Ground Surfaces and Its Impact on Fatigue Life. *CIRP Annals* 2006; 55:1. p. 81-84.
- [5] Tonshoff HK, Ardent C, Ben Amor R. Cutting of Hardened Steel. *CIRP Annals Manufacturing Technology* 2000; 49:2. p. 547-566
- [6] Ramesh A, Melkote SN, Allard LF, Riestler L, Watkins TR. Analysis of white layers formed in hard turning of AISI 52100 steel. *Materials Science and Engineering: A* 2005; 390:1–2. p. 88-97.
- [7] Akcan S, Shah WS, Moylan SP, Chhabra PN, Chandrasekar S, Yang HTY. Formation of white layers in steels by machining and their characteristics. *Metall Mater Trans A* 2002;33. p. 1245–1254.
- [8] Barry J, Byrne G. TEM study on the surface white layer in two turned hardened steels. *Materials Science and Engineering: A* 2002;325:1–2. p. 356-364.
- [9] Hosseini SB, Klement U, Yao Y, Rytberg K. Formation mechanisms of white layers induced by hard turning of AISI 52100 steel. *Acta materialia* 2015;89. p. 258-267.
- [10] Bartarya G, Choudhury SK. State of the art in hard turning. *International Journal of Machine Tools and Manufacture* 2012;53-1. p. 1-14.
- [11] Chincharikar S, Choudhury SK. Machining of hardened steel - Experimental investigations, performance modeling and cooling techniques: A review. *International Journal of Machine Tools and Manufacture* 2015;89. p. 95-109.
- [12] Edenhofer B, Joritz D, Rink M, Voges K. 13 - Carburizing of steels. *Thermochemical Surface Engineering of Steels*. Woodhead Publishing; 2015. p. 485-553.
- [13] Yi HY, Yan FK, Tao NR, Lu K. Work hardening behavior of nanotwinned austenitic grains in a metastable austenitic stainless steel. *Scripta Materialia*. Volume 114, 2016. p.133-136.
- [14] Hotz H, Kirsch B. Influence of tool properties on thermomechanical load and surface morphology when cryogenically turning metastable austenitic steel AISI 347. *Journal of Manufacturing Processes* 2020;52. p. 120-131.
- [15] Hosseini SB. White Layer Formation during Hard Turning of Through-Hardened Martensitic and Bainitic AISI 52100 steel. PhD thesis 2015.
- [16] Ding R, Knaggs C, Li H, Li YG, Bowen P. Characterization of plastic deformation induced by machining in a Ni-based superalloy. *Material Science and Engineering: A* 2020;778.
- [17] Hosseini SB, Beno T, Klement U, Kaminski J, Rytberg K. Cutting Temperatures During Hard Turning – Measurements and Effects of White Layer Formation in AISI 52100. *Journal of Materials Processing Technology* 2014;214. p. 1293–1300.
- [18] Hosseini SB, Klement U. A descriptive phenomenological model for white layer formation in hard turning of AISI 52100 bearing steel. *CIRP Journal of Manufacturing Science and Technology* 2021;32. p. 299-310.
- [19] Litovchenko IY, Tyumentsev AN, Akkuzin SA, Naiden EP, Korznikov AV. Martensitic transformations and the evolution of the defect microstructure of metastable austenitic steel during severe plastic deformation by high-pressure torsion. *Phys. Metals Metallogr* 2016;117. p. 847–856.
- [20] Hidalgo J, Findley KO, Santofimia MJ. Thermal and mechanical stability of retained austenite surrounded by martensite with different degrees of tempering. *Materials Science and Engineering: A* 2017;690. p. 337-347.
- [21] Bosheh SS, Mativenga PT. White layer formation in hard turning of H13 tool steel at high cutting speeds using CBN tooling. *International Journal of Machine Tools and Manufacture* 2006;46. p. 225-233.
- [22] Banerjee RL. X-ray determination of retained austenite. *J. Heat Treating* 1981;2. p. 147–150.